

Optimization of Air-gap Profile in Interior Permanent Magnet Synchronous Motors for Torque Ripple Mitigation

Jingchen Liang¹, Amir Parsapour¹, Zhuo Yang¹, Carlos Caicedo-Narvaez¹, Mehdi Moallem², *Senior Member IEEE*, and Babak Fahimi¹, *Fellow, IEEE*

¹ The University of Texas at Dallas, Department of Electrical and Computer Engineering, Richardson TX, USA
² Isfahan University of Technology, Department of Electrical and Computer Engineering, Isfahan, Iran

Corresponding author: Jingchen Liang, *Student Member, IEEE*
Postal address: 800 W Campbell Rd, ECSN 3.324, Richardson, TX 75080
Tel: 469-305-9239
Email: jxl146930@utdallas.edu

Abstract— Interior permanent magnet synchronous motors (IPMSMs) have been widely used due to their high efficiency and high power density. Minimization of torque pulsation resulting in vibration and acoustic noise is one of the important design considerations for IPMSMs. In this paper, a grid on/off search method for the rotor profile is proposed to mitigate torque pulsation. Selection of the rotor profile is due to the fact that air-gap is the most sensitive parameter in electric machines wherein changes in flux densities can cause substantial differences in the distribution of forces. A layer comprised of 20 partitions with a 0.1 mm thickness and 3 degrees wide grids have been introduced to the rotor surface for each pole and the possible geometries have been analyzed using finite element method (FEM) in ANSYS Maxwell. An optimal design was found that has the lowest torque ripple with a higher average torque compared to the original design. Genetic algorithm (GA) has also been applied to the method to automate the coupling between Maxwell and Matlab thereby saving the simulation time. Complete structural analysis has been done for both of the original and optimal designs to verify the superiority and feasibility of the proposed design.

Index Terms—Air-gap optimization, genetic algorithm, IPMSM, torque ripple.

This topic has been submitted as a digest to The Eighteenth Biennial IEEE Conference on Electromagnetic Field Computation (CEFC) 2018 and got accepted.

I. INTRODUCTION

INTERIOR permanent magnet synchronous motors (IPMSMs) have broad applications in electric vehicles, home appliances, and robotics due to their high power densities, high torque densities and large speed ranges [1], [2]. Permanent magnets are buried inside of the rotor, which leads to an unequal permeability for d -axis and q -axis leading to magnetic saliency. Given the presence of reaction torque, caused by the magneto-motive force (MMF) of the stator and its interaction with permanent magnets, the torque of IPMSM is a combination of reaction and reluctance torques, which provides a higher torque density and wider speed range during field weakening compared to other conventional machines [3].

However, torque pulsation is one of the most important design considerations in IPMSMs, since it can cause unwanted byproducts such as vibrations and acoustic noise. Mitigation of torque pulsation has been studied by many scholars. There are mainly two categories of methods, namely control techniques such as the current profiling method [4], [5], and the optimal design method. However, reducing torque pulsation based on power electronics and control method heavily depends on the accuracy of the power electronics circuits as well as the need for high end microcontrollers to guarantee a timely execution of the control algorithm. This paper proposes a torque ripple minimization method from the design point of view. Many techniques have addressed this topic, such as rotor or stator skewing [6]-[8], magnet skewing and shape optimization [7], slot/pole number combinations [7], [9], [10], optimization of flux barrier such as asymmetric flux barriers [11], rotor shape optimization, such as Kioumars *et al.* reported an optimal shape design obtained by drilling small circular holes in the rotor [12]-[14], and unequal air-gap length optimization [15]-[18].

The main purpose of air-gap profile optimization is to re-distribute the flux density and force components on the rotor surface with a smoother profile while keeping the average air-gap flux and torque density constant. Therefore, in this paper, a grid on/off search method on the rotor surface is introduced to optimize the air-gap profile such that not only the torque pulsation is mitigated but also the average torque and overall performance of the motor are improved. Grid on/off search method is implemented by introducing a layer of grids on the rotor surface, the material of each partition can be assigned as either air or iron, represented as “0” and “1” in the simulation process, which is similar as turning on and off switches in digital logic. Multiple simulations are executed, and their results are compared in order to search for an optimal combination of partitions to meet the optimization goal.

Furthermore, in order to reduce the simulation time, Genetic Algorithm (GA) is applied to this method. In the

optimization process, software Maxwell has been coupled to Matlab to automate the simulation process. Simulation results using finite element method (FEM) in ANSYS Maxwell as well as the structural analysis in ANSYS Workbench are presented for both the original and optimal designs to validate the feasibility of the optimal design.

The remainder of the paper is organized as follows, section II presents the analytical model for IPMSMs and the two dimensional (2D) model constructed in ANSYS Maxwell for this design. Section III introduces the grid on/off search method and the genetic algorithm applied thereto. Section IV presents the simulation results for both the original and the optimal designs. The structural analysis will be discussed in section V.

II. IPMSM MODEL

In order to understand the influence of the air-gap profile on torque pulsations in IPMSMs, it is necessary to construct the analytical model of the IPMSM and set up the model in ANSYS Maxwell for finite element analysis (FEA). In subsection A, the basic analytical model of IPMSM is introduced, and in subsection B, the 2D model which is built in ANSYS Maxwell is presented.

A. Analytical Model

The average electromagnetic torque for IPMSMs is well established as given in (1), which is a combination of the reaction torque and the reluctance torque [19].

$$T = \frac{3}{2}p(\lambda_{PM}i_q + (L_d - L_q)i_d i_q) \quad (1)$$

The total resultant torque of IPMSM can be viewed as an average torque and a pulsating torque which causes the torque ripple. The pulsating torque is mainly caused by three sources. The first source is the filed harmonic torque due to the nonideal sinusoidal distribution of the flux density in the air-gap. The second source is the cogging torque caused by the reluctance torque that exists between the permanent magnets and the stator teeth, and the third source is the reluctance torque generated by the inequality of the d -axis and q -axis inductances, which is indicated in the second term of equation (1) [13]. According to the above analysis, the flux distribution can directly affect the quality of the total torque in the machine. It is therefore necessary to analyze the air-gap profile (the rotor surface shape in this case) so that an optimal design for the rotor with minimum pulsation can be obtained.

B. 2D Model in ANSYS Maxwell

A 2D model, of a 1 hp, three-phase, 6 poles IPMSM has been constructed in the ANSYS Maxwell to validate the

torque ripple since cogging torque is caused by the interaction between the magnetic field of permanent magnets and the stator slots which depends strongly to the slot opening/slot pitch ratio [7]. It is important to note that in the presence of a slot-free stator and round rotor surface there are no cogging torque. Hence if an equivalent airgap length representing the impact of the slot opening can be found, it can be used as a step towards reducing/eliminating the cogging torque. To this end one can note that the relationship between slot opening and air-gap length can be described by Carter's coefficient [21], [22] which determines an effective air-gap length to obtain the MMF across the air-gap. This equivalent airgap approximates the airgap of a slot-free stator which generates the same MMF as observed in the real stator. The Carter's coefficient for this motor is obtained by (2) [23]:

$$C_S = \frac{w_{ss} + w_{st}}{w_{st} + \frac{4g}{\pi} \ln \left(1 + \frac{\pi w_{ss}}{4g} \right)} \quad (2)$$

Where w_{ss} is the stator slot width (4.86 mm), w_{st} is the stator tooth width (2.49 mm), and g is the air-gap length (0.75 mm). The effective air-gap length g' is calculated according to (3) [23], which is 0.9 mm.

$$g' = gC_S \quad (3)$$

Applying the above formulae to the machine under consideration will result in a difference of 0.15 mm layer on the rotor surface which leads to less cogging torque. In fact if the surface of the rotor is sculptured according to the slot opening using the Carter coefficient one would expect to remove the cogging torque entirely. However, this computation would be valid for one rotor position and over a complete electrical cycle various permutations of rotor surface is needed. Taking into account the impact of commutation torque and its addition to torque pulsation one needs to perform an optimization through comprehensive numerical simulation to find an ideal surface profile. This has been the underlying principle of our optimization philosophy. Furthermore, due to manufacturing limitations, the precision is limited to 0.1 mm. Meanwhile, as air-gap length increasing, the average torque would be punished. In this case, the thickness of 0.1 mm of the grid on the rotor surface is selected.

In this paper a layer of 20 partitions with a thickness of 0.1 mm and an angular span of 3 degrees have been introduced to the rotor surface for each pole. The number of partitions is chosen according to the angle of each pole (60 degrees) such that each partition has an integer angle. Simulation time also restricts the number of partitions since the number of all the combinations is an exponential growth according to the number of partitions, too many partitions would consume much more time.

In each iteration, 20 partitions can be combined with different permutations of air and iron. Thanks to symmetry,

the layout of 20 partitions is symmetric for each pole, so that all the possible permutations for only 10 partitions for half of a pole are simulated in Maxwell at the rated operating point. A sample rotor profile with a hybrid combination of the air and iron is shown in Fig.3 as an example. The material of each partition can be assigned as either air or iron, represented by “0” and “1” (shown in red and white in Fig.3 respectively.). Fig.4 illustrates the average torque versus torque ripple plot and notably an optimal region can be distinguished in which the lowest torque ripple and higher average torque is achieved.

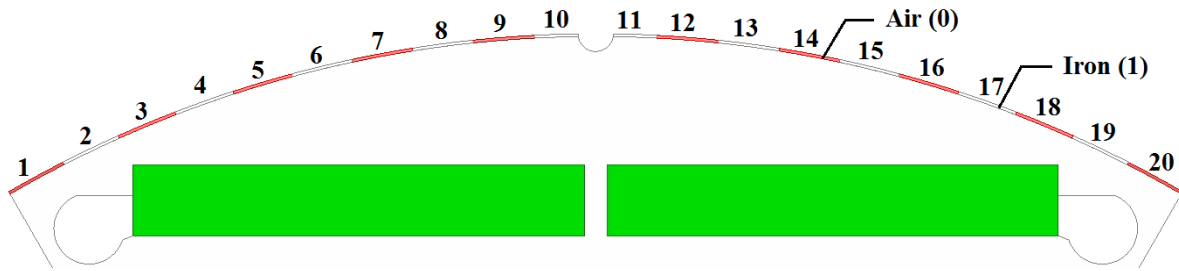


Fig. 3. A sample rotor profile with a hybrid combination of the air and iron partitions

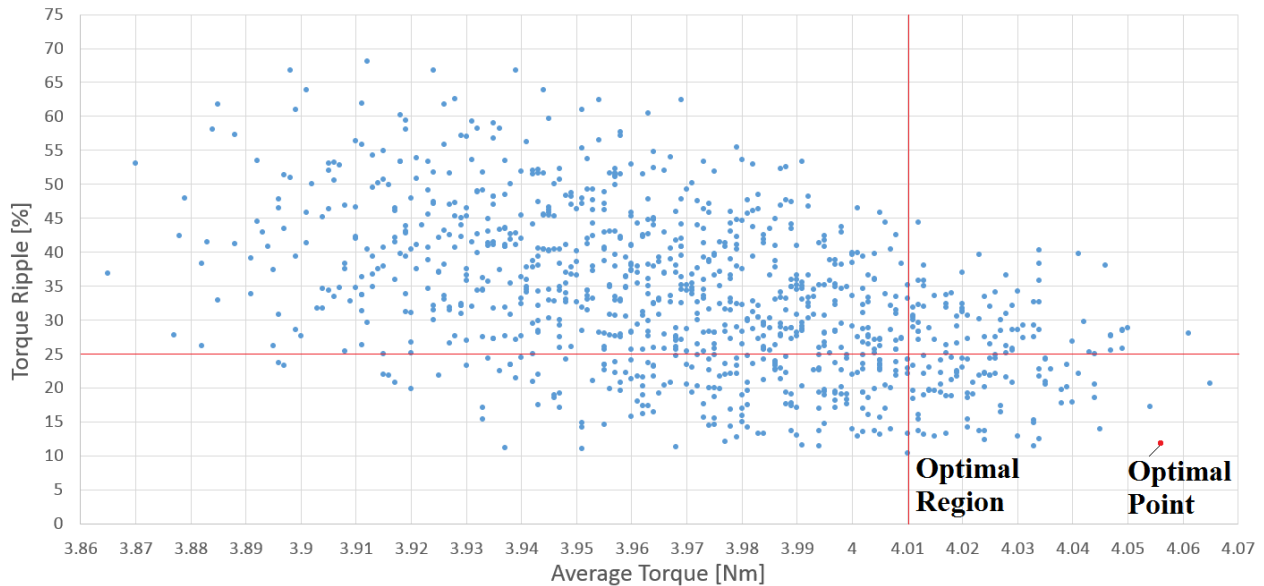


Fig. 4. Average torque vs. torque ripple

B. Genetic Algorithm

In order to reduce simulation time as well as the engineering effort, the GA tool box in Matlab has been used to assist with optimization method. This combination helps to find the global minimum for the targeted objective function.

Matlab has been coupled with ANSYS Maxwell through the Visual Basic Script exported from Maxwell to automate the simulation process. In each iteration, Matlab command controls Maxwell to execute the simulation, and

the torque information is exported in Excel files and loaded into Matlab. GA analyzes the data and decides if it gives the desired minimum value, if it does, the simulation terminates, and the minimum value as well as the optimal design variables will be recorded. Otherwise, GA will provide a new group of design variables for the combination of “0”s and “1”s for 10 partitions and rewrite them in the script to execute another iteration of the Maxwell simulation until it finds the global minimum. Population size, maximum number of generations, and chromosome length are set to 100, 10, and 10 respectively. The flow chart in Fig.5 shows the overall optimization process.

The objective function in this case is to minimize the torque ripple and to maintain or exceed the average torque with respect to the original design. As GA always searches for the minimum value, the objective function is defined as:

$$F = K_1 \left(\frac{T_{max} - T_{min}}{T_{avg}} \right) + K_2 \frac{1}{T_{avg}} \quad (4)$$

T_{max} , T_{min} , and T_{avg} are the maximum, minimum, and average torque respectively. K_1 and K_2 are the weights for torque ripple and the reciprocal of average torque, depending on which part is more important for the optimization due to application requirements. Since minimizing torque ripple and maximizing average torque have the same importance in this case, K_1 and K_2 both are set to be 0.5. The input variable, shown in (3), is a vector (i.e. chromosome) of the possible materials for 10 partitions, which is either air or iron represented by “0”s and “1”s.

$$X = [X_1 X_2 \dots X_{10}] \quad (5)$$

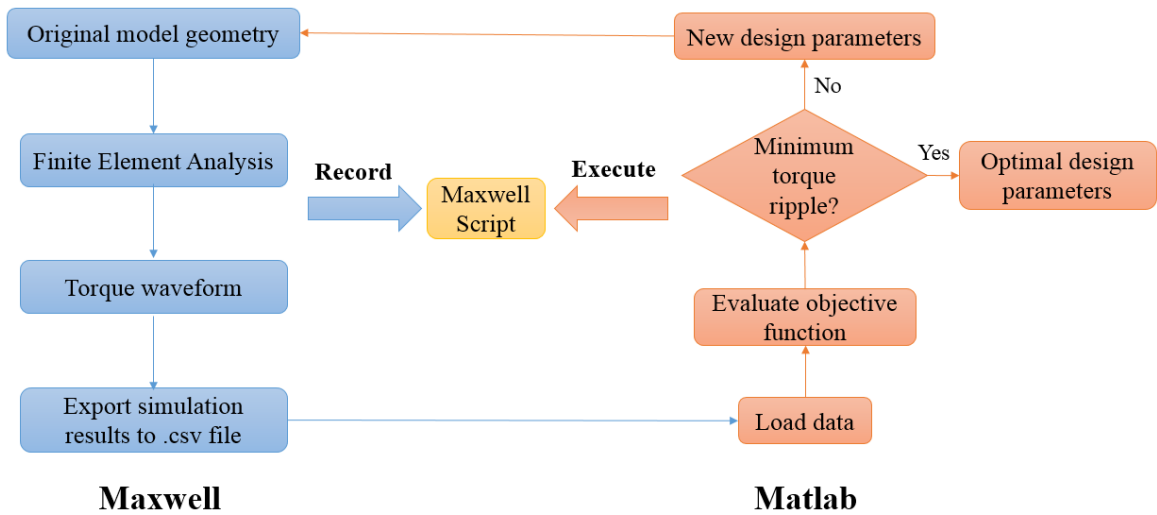


Fig. 5. Overall design optimization flow chart

IV. SIMULATION RESULTS

The optimal design of the rotor surface is obtained and the input variable of the optimal design detected by the

proposed method is given by:

$$X = [0\ 0\ 0\ 0\ 1\ 1\ 1\ 1\ 1\ 0] \quad (6)$$

Comparison of the original and the optimal designs of the rotor surface is shown in Fig.6. It must be noted that structural dimensions such as the outer diameter and inner diameter of stator, the outer diameter of rotor, the minimum air-gap length, and the stack length for original and optimal designs are all the same. The only difference between these two designs is the original rotor surface is smooth and has a constant radius, while the optimal rotor has unequal radius by 0.1 mm difference.

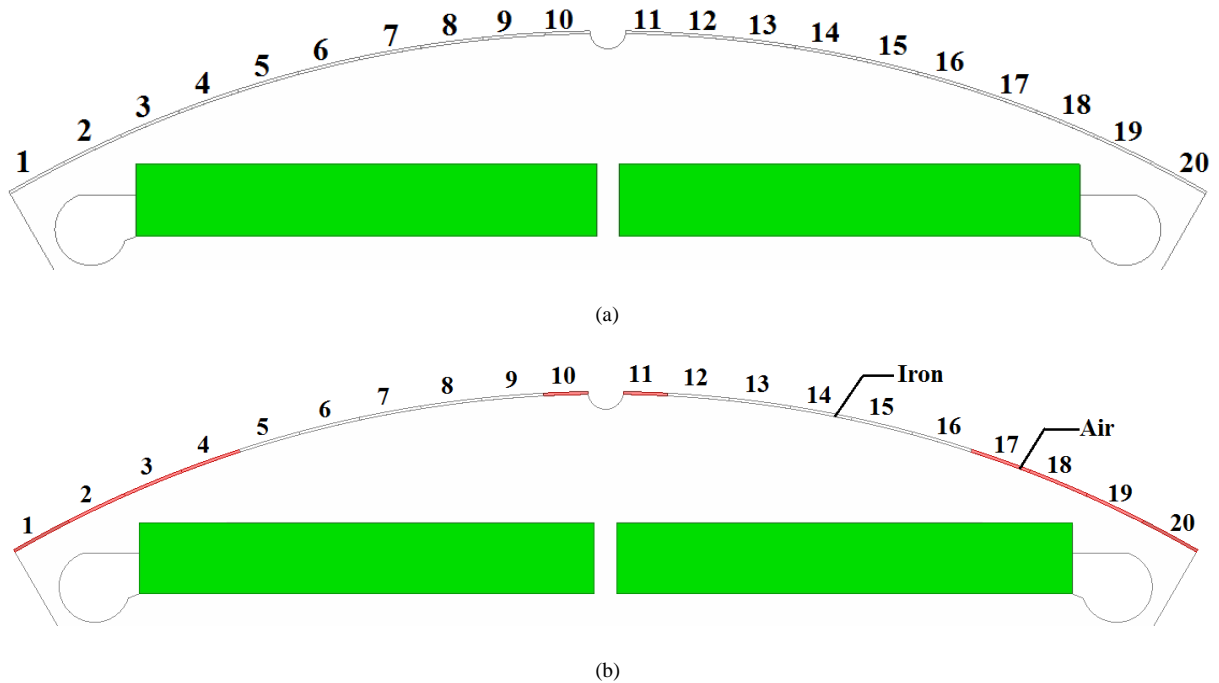


Fig. 6. (a) Original and (b) optimal rotor designs

Complete study including the torque performances, flux densities in the stator and air-gap, the tangential and radial forces acting on the rotor surface and the stator teeth, as well as the structural analysis has been done for both of the original and optimal designs to verify the feasibility of the proposed method as well as the optimal structure. All the simulation results are obtained at the rated operating point shown in TABLE I. Three-phase sinusoidal currents with 1.2 A root mean square (RMS) value and 120 degree phase shift are applied to excite the machine for both of the original and optimal designs.

A. Torque performance analysis

Fig.7 shows the comparison of the torque waveforms of the original and the optimal designs. Torque ripple was

significantly reduced from 27.56% to 12.05% which represents a 56.27% reduction. The average torque is increased from 4.01 Nm to 4.05 Nm which indicates a 1.12% of increase. This comparison indicates that the grid on/off search method for the optimal air-gap profile is practical for torque pulsation mitigation. Not only the torque ripple is effectively reduced, but also the average torque is slightly increased. The data comparison is concluded in TABLE II.

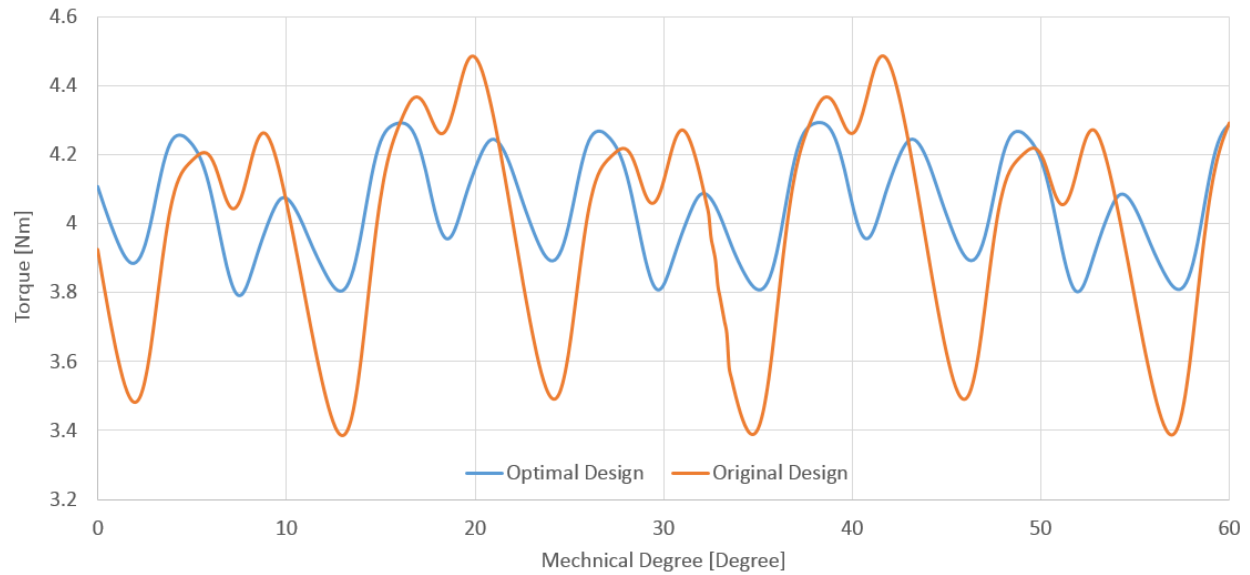


Fig. 7. Comparison of the original and the optimal torque waveforms

TABLE II
DATA COMPARISON OF THE ORIGINAL AND THE OPTIMAL TORQUE

	Original	Optimal	Comparison
Average Torque	4.01 Nm	4.05 Nm	1.12% ↑
Torque Ripple	27.56%	12.05%	56.27% ↓

B. Flux density in the stator

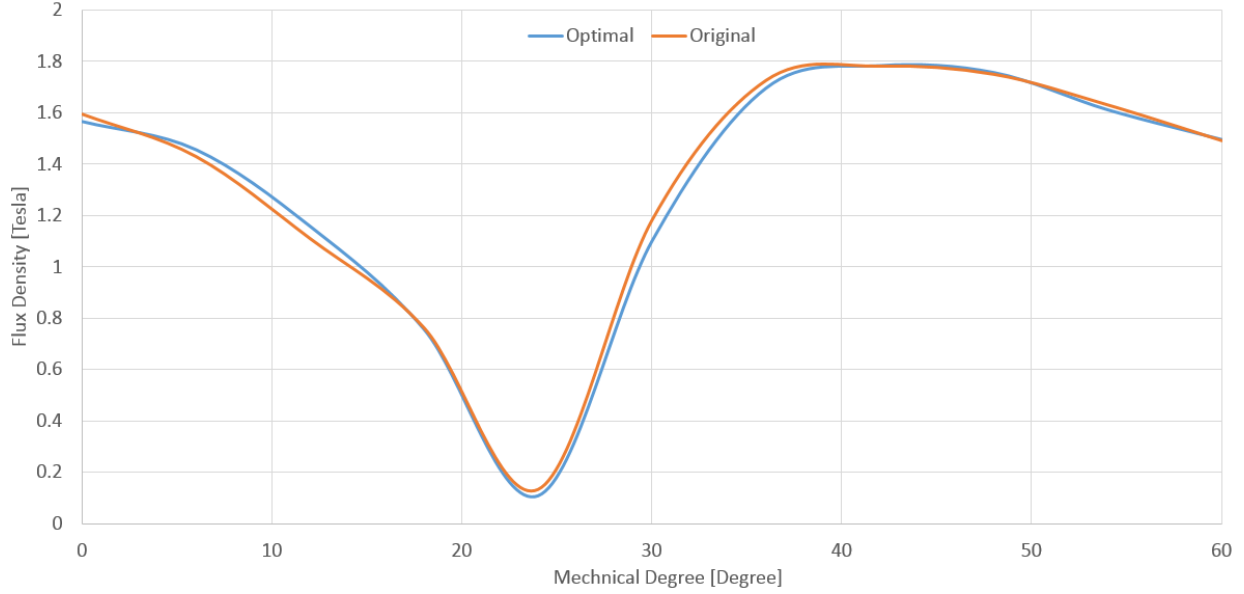


Fig. 8. Flux density in the stator teeth versus the rotor position for one pole

Fig. 8 shows the flux density in one of the stator teeth according to the rotor position for one electrical cycle for both of the original and optimal designs. The highest point of the flux densities for both of the designs are around 1.78 T. Since the core material of rotor and stator is silicon steel M-15, no saturation occurs in either of the designs. It is also expected that the core losses in both cases to be very similar.

C. Flux densities in the air-gap and tangential force on the rotor surface

The tangential force acting on the rotor surface has been analyzed. These forces contribute to the torque production and are desired to be larger. The normal and tangential flux densities B_n and B_t are calculated in Maxwell which are shown in Fig.9 and Fig.10 respectively can be used to calculate the tangential force density using Maxwell stress tensor [24], [22]:

$$f_t(\theta_r) = \frac{B_n(\theta_r)B_t(\theta_r)}{\mu_0} \quad (7)$$

where μ_0 is the air permeability constant, and θ_r is the position of the rotor surface, θ_r spans over a range of 60 degrees for each pole. Fig.11 shows the tangential force densities on the rotor surface for both original and optimal designs for each pole. The average tangential force density of the original design is 132.5 N/m² higher compared to the optimal design, which contributes to a higher average torque. Total torque can be calculated using (5) [25]:

$$T_e = 6 \sum_{\theta_r=0}^{60} \frac{1}{\mu_0} B_{n,\theta_r} B_{t,\theta_r} r^2 l \Delta\theta_r \quad (8)$$

where B_{n,θ_r} and B_{t,θ_r} are the radial and tangential flux densities on the rotor surface at certain angle θ_r , r is the rotor radius and l is the total stack length. The calculated average torque for original and optimal designs are 4.08 Nm and 4.15 Nm, both of the results are slightly higher than the simulation results, which is due to the difference of the FEM and the Maxwell stress tensor. However, both results indicate that the optimal design provides higher average torque than the original design.

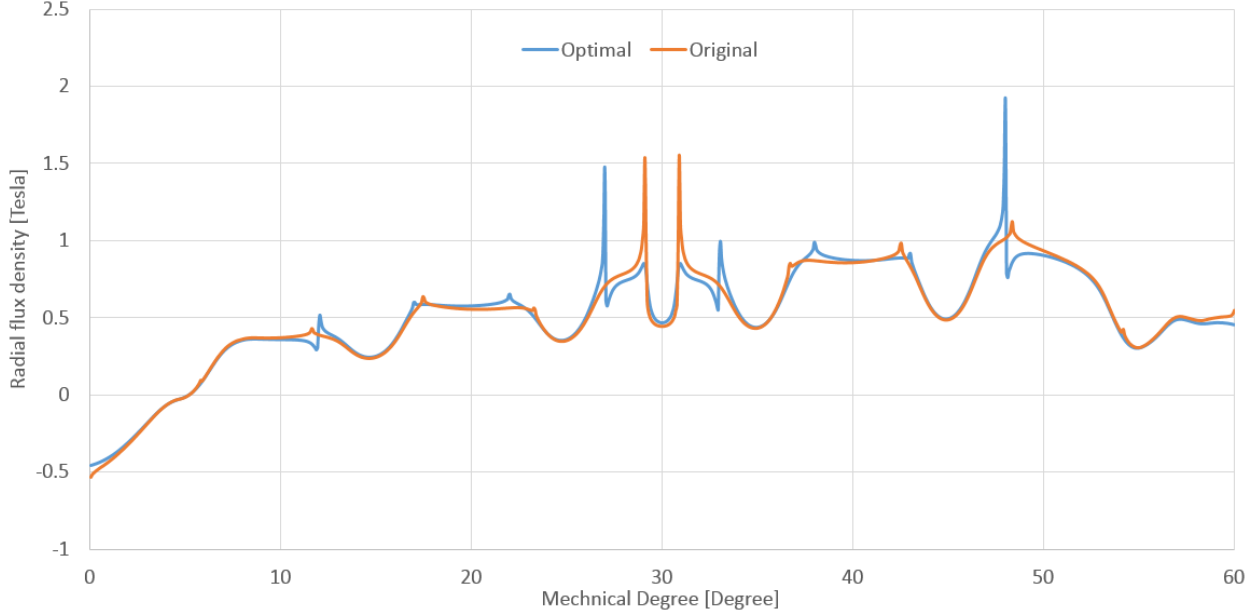


Fig. 9. Radial flux densities in air-gap for original and optimal designs

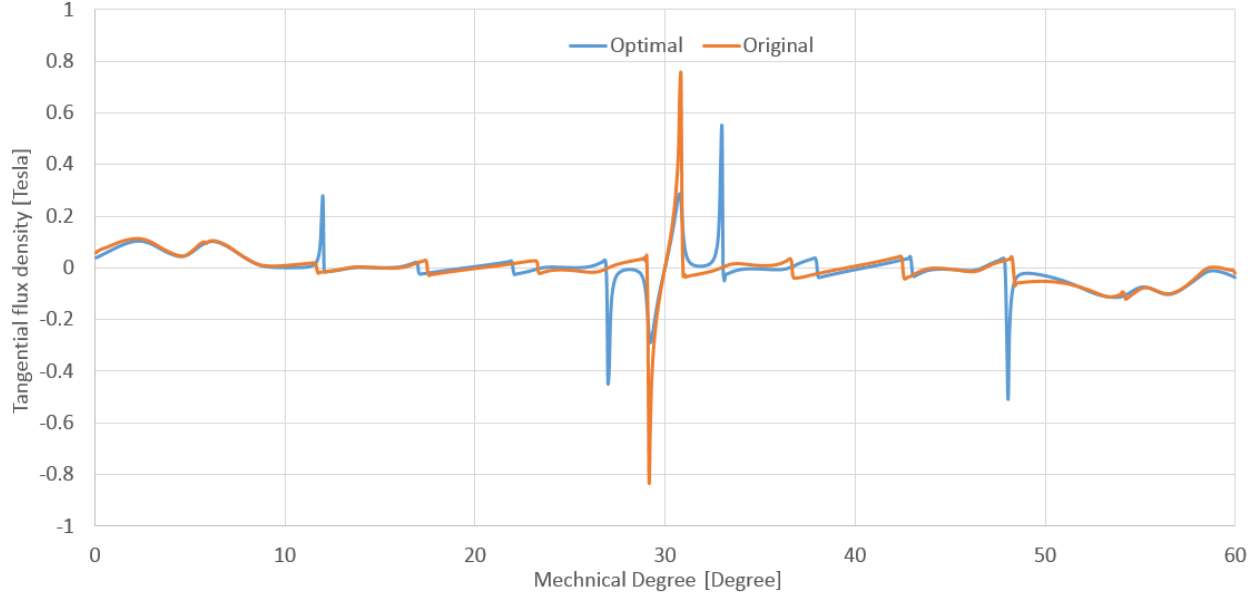


Fig. 10. Tangential flux densities in air-gap for original and optimal designs

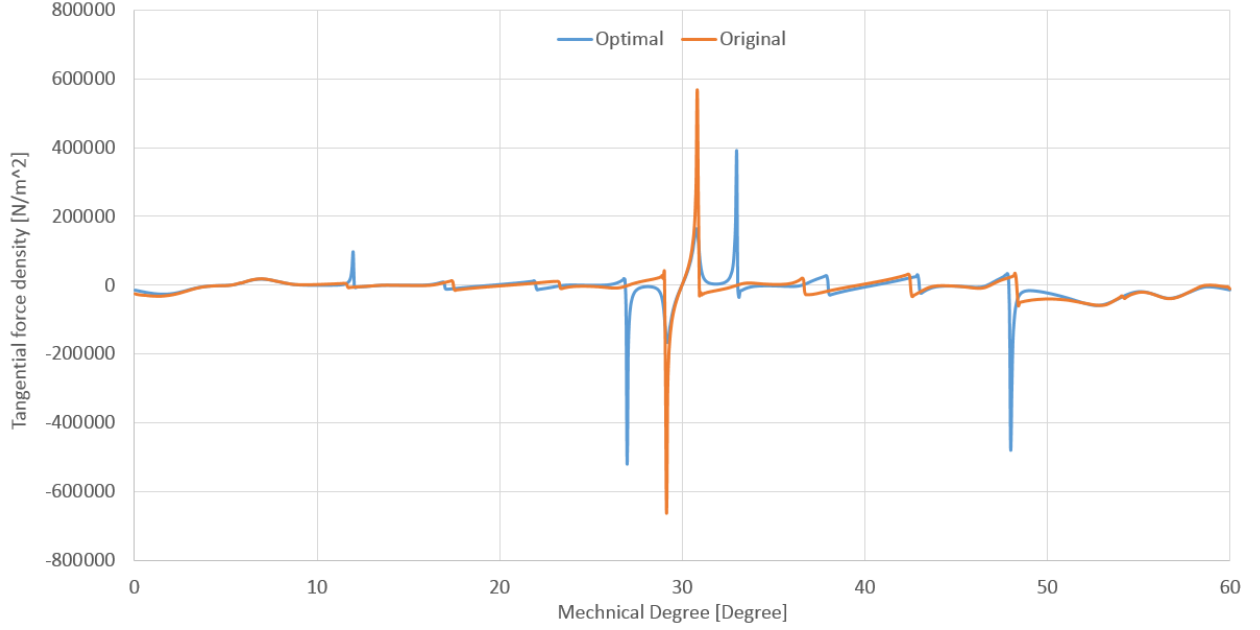


Fig. 11. Tangential force densities for original and optimal designs

V. STRUCTURAL ANALYSIS

It is important to check if the optimal design is structurally reliable. The static structural analysis in ANSYS Workbench has been performed on the stator by applying the calculated radial forces on the surfaces of the stator teeth in order to explore the total deformation and the equivalent stress caused by the vibration for both designs.

A. Radial forces acting on the stator teeth

Radial forces acting on the stator teeth are the main source of the vibration in the stator which contribute to acoustic noise [26]. The radial forces on the stator teeth can be calculated according to (10) [24], [25]:

$$f_r(\theta_s) = \frac{B_n(\theta_s)^2 - B_t(\theta_s)^2}{2\mu_0} \quad (9)$$

θ_s is the position angle on the surface of the stator teeth. Fig. 12 shows the radial force density acting on the stator teeth versus the mechanical degree of the stator teeth and slots for one pole. The optimal design has slightly lower magnitude than the original design such that radial forces acting on the stator for the optimal design are less, and the vibration as well as the acoustic noise will be smaller compared to the original design.

TABLE III
RADIAL FORCES ACTING ON STATOR TEETH

Stator tooth	Radial force (Original design)	Radial force (Optimal design)
1	533.4 N	380.1 N
2	247.5 N	265.4 N
3	829.5 N	741.2 N
4	1178.8 N	1131.3 N
5	1816.7 N	1691.0 N
6	1767.2 N	1676.5 N

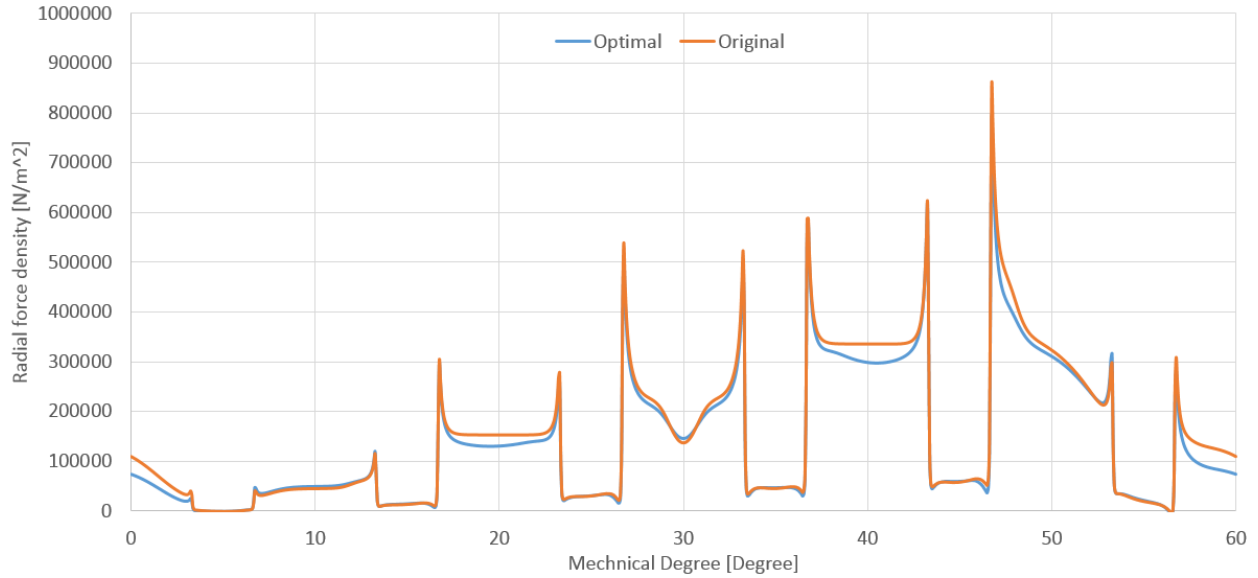


Fig. 12. Radial force densities for original and optimal designs

B. Structural Analysis

Forces acting on each stator tooth can be calculated by integrating the force density on the stator teeth surface. The calculated forces for six teeth of each pole for both the original and optimal designs under rated operating point are listed in TABLE III. The radial forces are calculated according to the radial force densities obtained from the Maxwell stress tensor. It is shown in Fig. 12 that the radial force density of second stator tooth of the optimal design is slightly higher than the original design, which causes a higher radial force acting on the stator teeth. Since the optimization goal is to reduce torque ripple and to increase average torque structural analysis is mainly for verifying the superiority and the feasibility of the proposed design, it is possible that one of the stator teeth has higher radial force than the original design. However, the overall performance of the optimal design is improved. Due to the symmetry, these forces can be applied to the stator teeth surface for all of the six poles under the rated operating point in structural analysis.

Fig. 13 shows the total deformation and equivalent stress of the stator under the applied radial forces on the stator

teeth for the original design. In this case, the maximum deformation is 0.008 mm, which is within the safe range as it is very small compared to the 0.75 mm air-gap length. The maximum equivalent stress is 28.7 MPa, which is within the safe range as the tensile yield strength for electric steel is about 358 MPa [27]. Fig.14 shows the same plots for the optimal design, the maximum value of the total deformation is decreased by 6.25%, which is 0.0075 mm, and the maximum value of the equivalent stress is also decreased by 7.32%, which is 26.6 MPa.

The structural analysis results indicate that the optimal design obtained by the proposed method not only reduced the torque pulsation and increased the average torque, but also reduced the radial forces acting on the stator teeth. In summary, it shows that the optimal design has better structural performance than the original design.

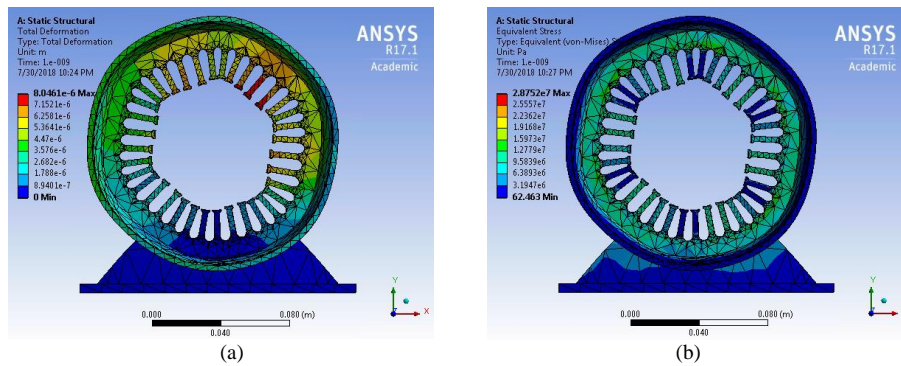


Fig. 13. Structural analysis for the original model (a) total deformation, (b) equivalent stress

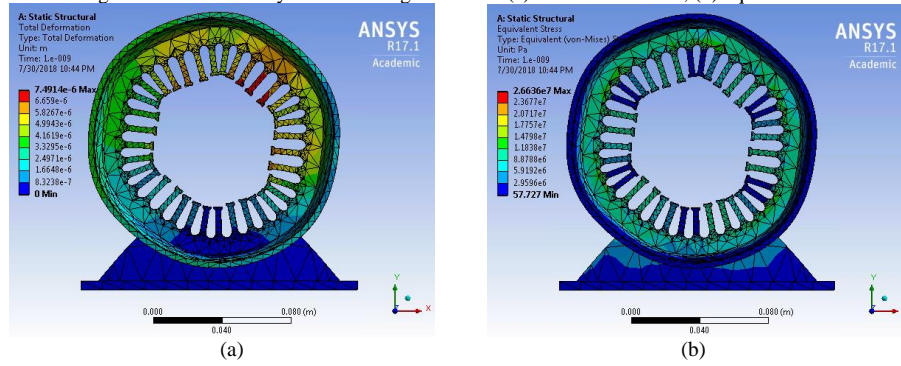


Fig. 14. Structural analysis for the optimal model (a) total deformation, (b) equivalent stress

VI. CONCLUSION

In this paper, a grid on/off search method optimization of the air-gap profile is proposed for mitigating the torque pulsation of an IPMSM motor. GA has been applied to this method to further reduce the simulation time. The FEM simulation results indicate that the optimal design reduces torque pulsation by 56.27% and increases average torque by 1.12%. Radial forces acting on the stator teeth are also reduced in the optimal design, thereby causing a reduction of the total deformation and the equivalent stress according to the structural analysis. This optimal rotor design is

easily applicable in the manufacturing process as compared to other rotor shape optimization methods.

REFERENCES

- [1] I. Boldea, L. Tutelea, *Electric Machines: Steady State, Transients, and Design with MATLAB*. Boca Raton, FL: CRC Press, 2009.
- [2] A. Emadi, *Energy-Efficient Electric Motors*, 3rd ed. Boca Raton, FL: CRC Press, 2004.
- [3] W. Wang, B. Fahimi and M. Kiani, "Maximum Torque per Ampere Control of Permanent Magnet Synchronous Machines," *2012 XXth International Conference on Electrical Machines*, Marseille, Sep 2, 2012, pp. 1013-1020.
- [4] L. Guo and L. Parsa, "Torque Ripple Reduction of the Modular Interior Permanent Magnet Machines Using Optimum Current Profiling Technique," in *Proc. IEEE IEMDC*, May 3–6, 2009, pp. 1094–1099.
- [5] G. H. Lee, S. I. Kim, J. P. Hong and J. H. Bahn, "Torque Ripple Reduction of Interior Permanent Magnet Synchronous Motor Using Harmonic Injected Current," in *IEEE Transactions on Magnetics*, vol. 44, no. 6, pp. 1582-1585, June 2008.
- [6] J. W. Jiang, B. Bilgin, Y. Yang, A. Sathyan, H. Dadkhah and A. Emadi, "Rotor Skew Pattern Design and Optimisation for Cogging Torque Reduction," in *IET Electrical Systems in Transportation*, vol. 6, no. 2, pp. 126-135, June 2016.
- [7] R. Islam, I. Husain, A. Fardoun and K. McLaughlin, "Permanent Magnet Synchronous Motor Magnet Designs with Skewing for Torque Ripple and Cogging Torque Reduction," in *IEEE Industry Applications*, vol. 45, no. 1, pp. 152-160, Jan.-feb. 2009.
- [8] H. Chen, D. G. Dorrell and M. Tsai, "Design and Operation of Interior Permanent-Magnet Motors With Two Axial Segments and High Rotor Saliency," in *IEEE Transactions on Magnetics*, vol. 46, no. 9, pp. 3664-3675, Sept. 2010.
- [9] S. Han, T. M. Jahns and W. L. Soong, "Torque Ripple Reduction in Interior Permanent Magnet Synchronous Machines Using the Principle of Mutual Harmonics Exclusion," in *IEEE Industry Applications Annual Meeting*, New Orleans, LA, Sep 23, 2007, pp. 558-565.
- [10] S. Han, T. M. Jahns and Z. Q. Zhu, "Design Tradeoffs Between Stator Core Loss and Torque Ripple in IPM Machines," in *IEEE Transactions on Industry Applications*, vol. 46, no. 1, pp. 187-195, Jan.-feb. 2010.
- [11] K. Kim, "A Novel Method for Minimization of Cogging Torque and Torque Ripple for Interior Permanent Magnet Synchronous Motor," in *IEEE Transactions on Magnetics*, vol. 50, no. 2, pp. 793-796, Feb. 2014.
- [12] A. Kiyomarsi and M. Moallem, "Optimal Shape Design of Interior Permanent-Magnet Synchronous Motor," *IEEE International Conference on Electric Machines and Drives*, San Antonio, TX, May 15, 2005, pp. 642-648.
- [13] A. Kioumarsi, M. Moallem and B. Fahimi, "Mitigation of Torque Ripple in Interior Permanent Magnet Motors by Optimal Shape Design," in *IEEE Transactions on Magnetics*, vol. 42, no. 11, pp. 3706-3711, Nov. 2006.
- [14] K. Yoon and B. Kwon, "Optimal Design of a New Interior Permanent Magnet Motor Using a Flared-Shape Arrangement of Ferrite Magnets," in *IEEE Transactions on Magnetics*, vol. 52, no. 7, pp. 1-4, July 2016.
- [15] K. Wang, Z. Q. Zhu, G. Ombach and W. Chlebosz, "Optimal Rotor Shape with Third Harmonic for Maximizing Torque and Minimizing Torque Ripple in IPM Motors," in *International Conference on Electrical Machines*, Marseille, Sep 2, 2012, pp. 397-403.
- [16] S. Chaithongsuk, N. Takorabet, B. Nahid-Mobarakeh and F. Meibody-Tabar, "Optimal Design of PM Motors for Quasi-sinusoidal Air-gap Flux Density," in *45th International Universities Power Engineering Conference (UPEC)*, Cardiff, Wales, Aug 31, 2010, pp. 1-6.
- [17] S. A. Evans, "Salient Pole Shoe Shapes of Interior Permanent Magnet Synchronous Machines," in *The XIX International Conference on Electrical Machines (ICEM) 2010*, Rome, Sep 6, 2010, pp. 1-6.
- [18] U. Seo, Y. Chun, J. Choi, P. Han, D. Koo and J. Lee, "A Technique of Torque Ripple Reduction in Interior Permanent Magnet Synchronous Motor," in *IEEE Transactions on Magnetics*, vol. 47, no. 10, pp. 3240-3243, Oct. 2011.
- [19] S. T. Lee and L. M. Tolbert, "Analytical Method of Torque Calculation for Interior Permanent Magnet Synchronous Machines," in *IEEE Energy Conversion Congress and Exposition*, San Jose, CA, Sep 20, 2009, pp. 173-177.
- [20] L. Gu, "Modeling of Permanent Magnet Machines Using Field Reconstruction Method," Ph.D dissertation, Department of Electrical and Computer Engineering, The University of Texas at Dallas, Richardson. Accessed on: Dec. 2016. [Online]. Available: <http://libtreasures.utdallas.edu/xmlui/handle/10735.1/5194>.
- [21] F. W. Carter, "The Magnetic Field of the Dynamo-electric Machine," *Journal of the Institution of Electrical Engineers*, vol. 64, no. 359, pp. 1115-1138, 1926.
- [22] O. Laldin, S. D. Sudhoff, and S. Pekarek, "Modified Carter's Coefficient," in *IEEE Transactions on Energy Conversion*, vol. 30, no. 3, pp. 1133-1134, Sept. 2015.
- [23] P. C. Krause, O. Wasynczuk, S. D. Sudhoff, and S. D. Pekarek, *Analysis of Electric Machinery and Drive Systems*, 3rd ed. Piscataway, NJ, USA, IEEE Press, 2013.

- [24] M. Kanematsu, T. Miyajima, H. Fujimoto, Y. Hori, T. Enomoto, M. Kondou, H. Komiya, K. Yoshimoto, and T. Miyakawa, "Radial force control of IPMSM considering fundamental magnetic flux distribution," in *IEEJ Journal of Industry Applications*, vol. 3, no. 4, pp.328-334, 2014.
- [25] W. Zhu, S. Pekarek, B. Fahimi and B. J. Deken, "Investigation of Force Generation in a Permanent Magnet Synchronous Machine," in *IEEE Transactions on Energy Conversion*, vol. 22, no. 3, pp. 557-565, Sept. 2007.
- [26] M. Krishnamurthy and B. Fahimi, "Qualitative Analysis of Force Distribution in a 3-phase Permanent Magnet Synchronous Machine," in *IEEE International Electric Machines and Drives Conference*, Miami, FL, May 3, 2009, pp. 1105-1112.
- [27] L. Maharjan, S. Wang, A. H. Isfahani, W. Wang and B. Fahimi, "Comparative Study of Structural Rigidity of Induction Machine and Switched Reluctance Machine," in *IEEE Transportation Electrification Conference and Expo (ITEC)*, Dearborn, MI, Jun 15, 2014, pp. 1-5.